

Microfabrication of Oxidation-Sharpended Silicon Tips on Silicon Nitride Cantilevers for Atomic Force Microscopy

Albert Folch, Mark S. Wrighton, and Martin A. Schmidt

Abstract—We have developed a novel process for the microfabrication of atomic force microscope (AFM) cantilevered tips from silicon-on-insulator (SOI) wafers. The tip and cantilever are made of crystalline silicon and low-stress silicon nitride, respectively. This choice of materials allows us to sharpen the tips by oxidation sharpening without affecting the cantilever. We evaluated their performance in contact mode during imaging of artificial nanostructures and compared them to commercially available ones. The images acquired with our tips feature superior resolution on those samples. [270]

Index Terms—Atomic force microscope, microfabricated cantilevers, microfabricated tips, silicon-on-insulator wafers.

I. INTRODUCTION

THE ATOMIC force microscope (AFM) [1] has become a powerful tool for investigating surfaces on an atomic or nanometer scale. An AFM consists of a sharp cantilevered tip that is scanned within nanometric proximity over a surface. The forces between the tip and sample cause a minute cantilever deflection, which is sensed to obtain a topographical map of the surface on a nanometer or atomic scale. Since its invention, the AFM has been used not only to view surface structures, but also to probe electrical, magnetic, van der Waals, adhesion, and chemical interactions between the tip and surface and to modify surfaces by means of those interactions (see, for example, [2] and references therein).

The sharpness of the tip is often a fundamental resolution-limiting parameter. When the tip and sample are in contact, the area of contact increases with the radius of curvature of the tip apex. During noncontact imaging, on the other hand, sharper tips can be brought into closer proximity with the surface before a jump-to-contact instability occurs [3]. Furthermore, the sample features appear widened or convoluted by the tip.

Microfabrication is necessary because it is desirable that the cantilever have low stiffness for higher sensitivity and high resonance frequency for better immunity to vibrations [4].

Manuscript received May 21, 1997; revised August 5, 1997. Subject Editor, R. B. Marcus. This work was supported by the National Science Foundation and the Direcció General de la Recerca, Catalonia, Spain, and Motorola, which supplied the SOI wafers.

A. Folch is with the Department of Chemistry and the Microsystems Technology Laboratory, Massachusetts Institute of Technology (MIT), Cambridge, MA 02139 USA (e-mail: afolch@mit.edu).

M. S. Wrighton was with the Department of Chemistry, Massachusetts Institute of Technology (MIT), Cambridge, MA 02139 USA. He is now with Washington University, St. Louis, MO 63130 USA.

M. A. Schmidt is with the Microsystems Technology Laboratory, Massachusetts Institute of Technology (MIT), Cambridge, MA 02139 USA.

Publisher Item Identifier S 1057-7157(97)08221-8.

However, silicon micromachining techniques used to make the cantilevered tip do not generally ensure nanometric sharpness of the tip. Marcus *et al.* [5], [6] observed the anomalous oxidation of crystalline Si at sharp edges and low temperatures (900°–950 °C) and used it to sharpen Si tips for field-emission devices. By repeatedly growing SiO₂ on the Si tips and stripping it with HF, they achieved <1-nm radii of curvature at the tip apex. Recently, Itoh *et al.* [7] implemented the concept of oxidation sharpening in AFM Si tips on SiO₂ cantilevers. Their process, however, is limited in the sense that the tip cannot be arbitrarily sharpened because dissolution of the oxide grown in the sharpening process attacks the cantilever. Therefore, their cantilevers cannot be arbitrarily thin, which rules out their process for the microfabrication of thin low-compliance AFM cantilevers. The same limitation applies to crystalline tips integrated onto crystalline Si cantilevers [8].

Here, we present in detail a simple process that allows us to microfabricate silicon nitride cantilevers with integrated Si tips, which can be arbitrarily sharpened without affecting the cantilever. Since the cantilever material is deposited, the thickness of the lever can be specified with great accuracy.

II. CANTILEVERED TIP FABRICATION

The process is sketched in Fig. 1. We start with a double-side polished silicon-on-insulator (SOI) wafer.¹ The front side of the SOI wafer consists of a 5- or 10- μm -thick (100)-oriented Si layer (which we call the “SOI layer”) on a 0.5–1- μm -thick buried SiO₂ film, which is grown on a \sim 500- μm -thick (100)-oriented handle wafer. The dopant type and concentration are not relevant to our process. The tip is created from the SOI layer, as explained below. The periodicity of the pattern (and therefore the size of the AFM cantilever chip) is 3500 μm \times 3600 μm . The process consists of four major steps: 1) bulk micromachining to create a silicon membrane; 2) plasma etch to create a bilayer cantilever; 3) wet isotropic etch to create a tip; and 4) oxidation sharpening of the tip.

In all photolithographic steps, positive photoresist was spun onto the wafer with thicknesses ranging from 1 to 7 μm , baked at 90 °C for 30–60 min, then exposed to UV light through a contact chrome mask, and developed and baked at 120 °C for 30–60 min. The patterns were transferred either onto silicon nitride or onto Si with a SF₆-based plasma etch or onto SiO₂ with a buffered HF etch. Photoresist is always removed by

¹Courtesy of Motorola, Inc.

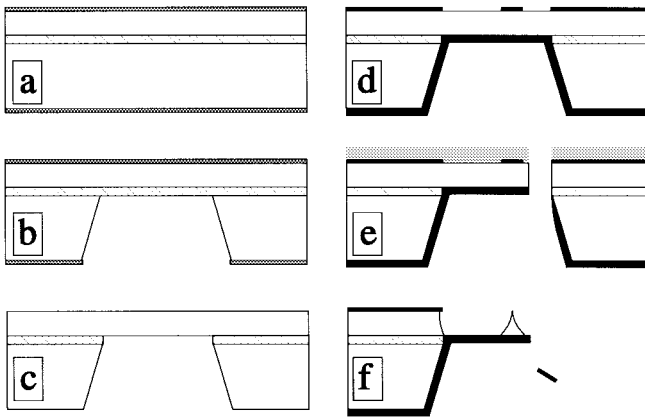


Fig. 1. Cross-sectional schematic representation of the wafer at each step of the microfabrication process (see text). In all drawings, the top corresponds to the wafer front side.

immersing the wafers in a piranha solution ($\text{H}_2\text{SO}_4:\text{H}_2\text{O}_2::3:1$) for 10 min.

A. Bulk Micromachining

To avoid wafer-edge erosion during the bulk micromachining step, we confine the pattern to an inner circle ~ 5 mm from the edge of the wafer. In addition, to help preserve the integrity of the wafer throughout the process and to enable handling of the wafer with vacuum wands, an area of ~ 3 cm² at the center of the wafer is not patterned.

First, a thin (~ 430 Å) stress-relief oxide (SRO) layer is thermally grown and low-pressure chemical vapor deposition (LPCVD) Si_3N_4 (~ 1500 Å) deposited on it [Fig. 1(a)]. The nitride/SRO layer is photolithographically patterned to expose rectangular areas ($975 \mu\text{m} \times 2600 \mu\text{m}$) of Si on the back side of the wafer. We use the wafer flat to align this mask with the crystallographic axis of the wafer. These exposed areas are etched in a 20% (% weight) potassium hydroxide and water (KOH) aqueous solution at 80°C , while the front side is protected from etching by the nitride/SRO layer. The measured etch rate is $\sim 90 \mu\text{m}/\text{h}$. Since SiO_2 etches ~ 100 times slower than $\text{Si}(100)$ [9], the etch stops when the buried SiO_2 layer is reached. Thus, the formed pit (as observed from the back side) has a flat bottom and (111)-oriented-inclined side walls characteristic of the anisotropic KOH etch [Fig. 1(b)]. We then proceed by selectively removing the nitride in a hot phosphoric acid bath (175°C , 45 min) and by dissolving both the exposed areas of the buried SiO_2 layer and the front-side SRO layer in buffered HF (5–10 min) [Fig. 1(c)]. At this point, the wafer consists of an array of bare crystalline-Si membranes of a thickness approximately equal to the starting SOI layer and $\sim 350 \mu\text{m} \times \sim 2000 \mu\text{m}$ in size. The exact size depends on the thickness of the starting wafer and does not affect our process.

B. Cantilever Pattern

The cantilever material, Si-rich nitride, is deposited on the wafers in an LPCVD furnace at 775°C and 280 mTorr with a mixture of SiH_2Cl_2 and NH_3 in a 10:1 flow ratio. The intrinsic stress of this material is ten times lower than that of stoichiometric nitride (Si_3N_4) [10]. Si_3N_4 films result in

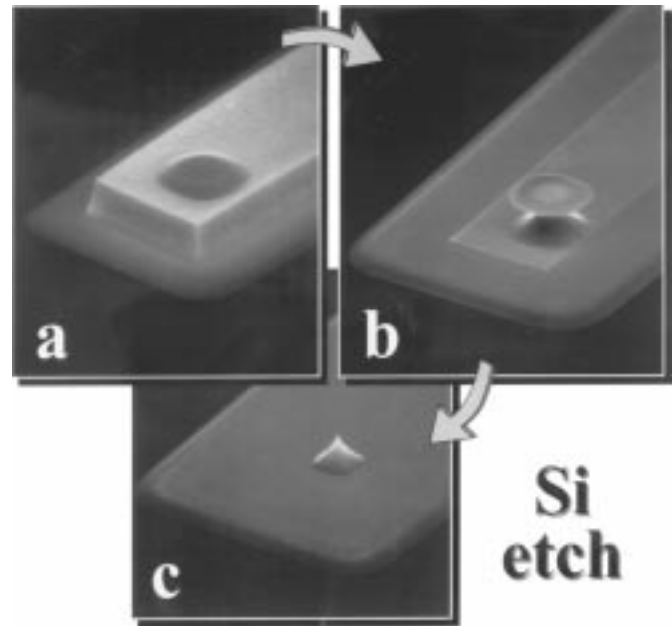


Fig. 2. SEM pictures depicting the formation of the cantilevered tip by isotropic etch of Si (light gray) in a 100:1 solution of $\text{HNO}_3:\text{HF}$, which does not attack silicon nitride (dark gray). The pictures show the cantilever (a) before, (b) during, and (c) after the Si etch.

curved cantilever beams, whereas our Si-rich nitride films do not, as shown below. Note that the membrane is coated with nitride on both sides and that it is strong enough to withstand the next two photolithography steps on its front side. First, a pattern of squares of photoresist ($10 \mu\text{m} \times 10 \mu\text{m}$ or $20 \mu\text{m} \times 20 \mu\text{m}$ for the 5- or 10- μm -thick SOI wafers, respectively) is defined on the membrane and transferred onto the front-side nitride layer with a high-power (250 W) SF_6 plasma etch [Fig. 1(d)]. Back-side illumination and an infrared camera are used to align this mask onto the membrane. The squares will later serve as a mask for the formation of the tip, but we proceed first to the cantilever formation step. The shape of the cantilever is defined on the front side of the membrane through a thick ($\sim 6 \mu\text{m}$) photoresist pattern (aligned onto the nitride square such that it is fully covered by the photoresist with its edge $\sim 5 \mu\text{m}$ away from the edge of the cantilever). A low-power (50 W) SF_6/CCl_4 plasma etch (10:1 $\text{SF}_6:\text{CCl}_4$ flow-rate ratio) is used to clear the membrane in the exposed Si areas [Fig. 1(e)]. The CCl_4 gas serves to selectively deposit a protective layer of carbonaceous polymer on the side walls as the etch proceeds, reducing undercuts and producing straight side walls [11]. Thus, a bilayer (nitride/Si) cantilever with a square nitride pattern is formed. A scanning electron microscope (SEM) picture of the device at this point of the process is shown in Fig. 2(a).

C. Tip Formation

The tips are formed by wet etch in a solution of 100:1 $\text{HNO}_3:\text{HF}$ solution, which etches Si ($\sim 0.5 \mu\text{m}/\text{min}$), but not silicon nitride [12], [13]. This etch isotropically undercuts a nitride square to form a tip. Hence, the tip mask is designed to be at least twice as large as the thickness of the starting SOI layer. In a typical 5- μm -deep Si etch, we measure a

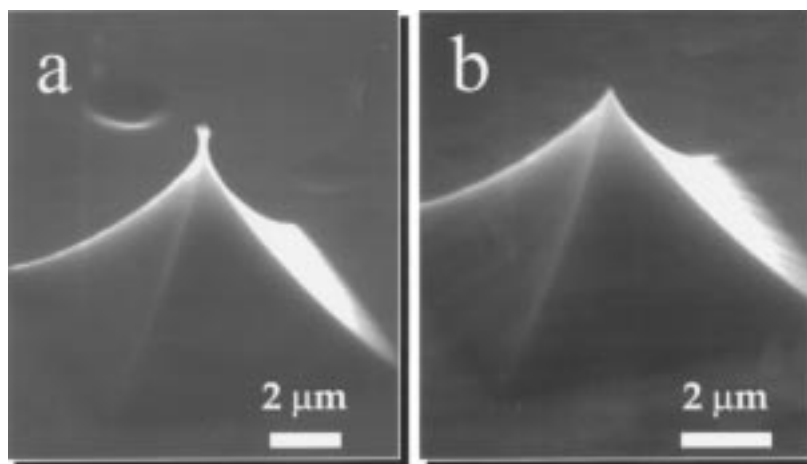


Fig. 3. SEM picture of a tip (a) before and (b) after a set of two oxidation-sharpening steps (see text).

~ 50 -Å (negligible for our purposes) Si-rich nitride etch. An SEM picture of an incomplete tip is shown in Fig. 2(b). When the back-side nitride layer is reached, the front-side $10\text{-}\mu\text{m} \times 10\text{-}\mu\text{m}$ nitride square has been undercut to a degree such that it is either supported by a thin ($< 1\ \mu\text{m}$) column or it is removed [Figs. 1(f) and 2(c)]. A finished tip typically has a front-side $\sim 8\text{-}\mu\text{m} \times 8\text{-}\mu\text{m}$ base and is $\sim 1\ \mu\text{m}$ lower than the starting thickness of the SOI layer. The etch rate ($\sim 0.5\text{--}1.5\ \mu\text{m}/\text{min}$) decreases with time, probably due to depletion of HF in the solution ($\sim 1\ \text{L}$), and is not uniform across the wafer. Therefore, most of the finished tips on the wafer, such as the one in Fig. 3(a), end in a submicron-sized platform or wedge or in a broken stem, and they must be sharpened in order to be suitable for AFM imaging.

To compensate for the nonuniformity of the etch, we designed our mask so that chips contain three cantilevers, each with slightly different ($1\ \mu\text{m}$) square sizes for the tip mask. Thus, at least one cantilevered tip on each chip was viable for imaging. We chose the wet etch for its simplicity and because it serves to demonstrate the powerful idea that a Si tip can be sharpened without affecting the nitride lever. Recently, Boisen *et al.* [14] obtained high yields in the formation of Si tips of various aspect ratios by reactive ion etch with SiO_2 masks. Our preliminary results, not shown here, similarly demonstrate a 95% yield in the formation of Si tips by pure SF_6 plasma etch with nitride masks. This dry etch can straightforwardly substitute the $\text{HNO}_3\text{:HF}$ etch in our process to allow for better control over the tip shape.

D. Oxidation Sharpening

We have followed well-known recipes for oxidation sharpening [5], [6]. We usually grow $\sim 500\ \text{nm}$ of thermal oxide at $950\ ^\circ\text{C}$ and strip it in buffered HF. In accordance with Marcus *et al.*, we observe that if the wedge or platform at the apex of a tip after the $\text{HNO}_3\text{:HF}$ etch is wider than a certain value ($\sim 500\ \text{nm}$ in our case), then the apex develops into two or four microtips, respectively, after oxidation sharpening. In our case, this occurs for $\sim 50\%$ of the tips due to the poor reliability and nonuniformity of the $\text{HNO}_3\text{:HF}$ etch process. However, all tips with an apex narrower than $500\ \text{nm}$ before the oxidation step(s)

develop a single microtip and, after two oxidation-sharpening steps, become indistinguishable from each other under SEM inspection. Since the radius of curvature at the tip apex is in most cases smaller than $10\ \text{nm}$, the resolution of our SEM does not allow us to measure it directly. Instead, as shown below, we tested the tips in AFM contact mode and demonstrated their superior sharpness when compared to commercially available ones. Each cycle of oxidation and dissolution results in a decrease in tip size. Typically, tips made from wafers with a $10\text{-}\mu\text{m}$ -thick SOI layer are $\sim 6\text{--}7\ \mu\text{m}$ tall after the two oxidation-sharpening steps.

III. AFM TIP TESTING

We have successfully imaged a variety of samples with AFM using our tips on $1\text{-}\mu\text{m}$ -thick cantilevers ($\sim 30\text{-kHz}$ resonance frequency) in contact mode. Thicker and stiffer ($> 100\ \text{kHz}$) cantilevers must be used for operation in noncontact mode.

In AFM, resolution is a sample-dependent concept: the ability to resolve atomic spacings on graphite or mica, for example, does not give information on the sharpness of the tip. Well-defined artificial nanostructures, such as KOH-etched $\sim 100\text{-nm}$ -deep pyramidal nanopits on Si(100) (see Fig. 4), are our preferred choice for evaluating lever performance and tip sharpness simultaneously. Tip-sample convolution, manifested in the form of features repeated over each nanostructure, allows us to infer qualitative information on the tip shape. Fig. 4(a) shows an AFM image of the pits (bottom) and an SEM image of the commercial tip² (top) used to acquire the AFM image. All the pyramids appear to have a flat inclined top and end in a ridge rather than a vertex. By comparison, the AFM image acquired with one of our oxidation-sharpened tips [Fig. 4(b)] features sharply pointed pyramids and pyramids with ridges oriented in either crystallographic direction, which is to be expected if the square mask for the KOH etch is not perfectly square [9]. The same differences between the two tips

²We used a Dimension 3000 by Digital Instruments at the C.M.S.E. (MIT) and the contact-mode tips (nominal force constant of $0.06\ \text{N/m}$) supplied with it. The force constant of our cantilevers was computed from data in [9] and well-known formulas for beam deflection.

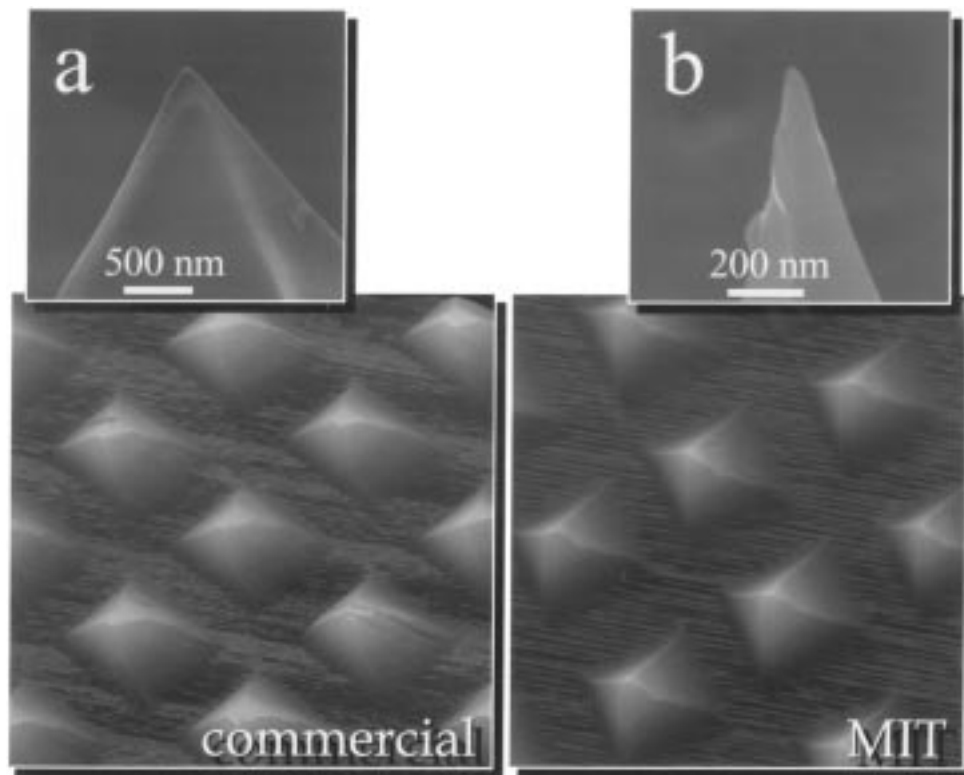


Fig. 4. SEM images of (top) (a) a commercial tip and (b) one of our tips after acquiring the corresponding (bottom) AFM contact-mode images of ~ 100 -nm-deep and 150 -nm-side pyramidal pits on Si. The AFM tip irregularities are attributed to wear during scanning. Imaging parameters were identical for both images: 10^{-9} N constant force, 4-Hz scan rate, and 600-nm scan range. For clarity, the AFM images are plotted in three-dimensional simulated illumination and inverted color scale, which causes the pits to appear as pyramids. Our AFM tips clearly feature less convolution.

were observed in other sample spots. The tip in Fig. 4(b) was not our sharpest, but one of the sharpest ones that survived scanning with similar imaging conditions [10^{-9} N applied force in both images (see the second footnote)]. Tips with a smaller radius of curvature at the apex apply more pressure for the same applied force and are thus more prone to fracture. Note the debris or particles on both tips not present before scanning and presumably due to wear during imaging.

IV. CONCLUSION

In summary, we have described in detail a novel process for microfabricating AFM low-stress silicon nitride levers with oxidation-sharpened Si tips. The novelty of our process is that both the sharpening procedure and the tip-formation step leave the cantilevers intact. Alternatively, one could implement the cantilever formation step at the end of the process to increase the tip viability yield in combination with a dry tip etch or to create Si tips on other low-stress materials. We have favorably compared our tips with the most widely used commercial tips during AFM imaging of demanding samples such as nanofabricated pyramidal pits.

ACKNOWLEDGMENT

We thank P. Tierney and T. Tyson (M.T.L.) for making the chrome masks, B. Alamariu (M.T.L.) for the low-stress nitride depositions, and A. Franke (N.S.L., MIT) for making the nanopits. We are grateful to L. Parameswaran, O. Hurtado, and L. Cordes (M.T.L.) for their insight and fruitful comments.

REFERENCES

- [1] G. Binnig, C. F. Quate, and Ch. Gerber, *Phys. Rev. Lett.*, vol. 56, no. 9, p. 930, 1986.
- [2] D. Sarid, *Scanning Force Microscopy*. New York: Oxford Univ. Press, 1991.
- [3] J. N. Israelachvili, *Intermolecular and Surface Forces*. London: Academic, 1985.
- [4] T. R. Albrecht, S. Akamine, T. E. Carver, and C. F. Quate, *J. Vac. Sci. Technol.*, vol. A 8, no. 4, p. 3386, 1990.
- [5] R. B. Marcus, T. S. Ravi, T. Gmitter, K. Chin, D. Liu, W. J. Orvis, R. D. Ciarlo, C. E. Hunt, and J. Trujillo, *Appl. Phys. Lett.*, vol. 56, no. 3, p. 236, 1990.
- [6] T. S. Ravi, R. B. Marcus, and D. Liu, *J. Vac. Sci. Technol.*, vol. B 9, no. 6, p. 2733, 1991.
- [7] J. Itoh, Y. Tohma, S. Kanemaru, and K. Shimizu, *J. Vac. Sci. Technol.*, vol. B 13, no. 2, p. 331, 1995.
- [8] J. Brugger, R. A. Buser, and N. F. de Rooij, *Sens. Actuators*, vol. A 34, p. 193, 1992.
- [9] K. E. Petersen, "Silicon as a mechanical material," *Proc. IEEE*, vol. 70, no. 5, p. 420, 1982.
- [10] B. Alamariu, private communication.
- [11] S. Wolf and R. N. Tauber, *Silicon Processing for the VLSI Era (Volume 1: Process Technology)*. Sunset Beach, CA: Lattice, 1986.
- [12] H. Robbins and B. Schwartz, *J. Electrochem. Soc.*, vol. 106, no. 6, p. 505, 1959.
- [13] ———, *J. Electrochem. Soc.*, vol. 107, no. 2, p. 108, 1960.
- [14] A. Boisen, O. Hansens, and S. Bouwstra, *J. Micromech. Microeng.*, vol. 6, p. 58, 1996.

Albert Folch, photograph and biography not available at the time of publication.

Mark S. Wrighton, photograph and biography not available at the time of publication.

Martin A. Schmidt, photograph and biography not available at the time of publication.